

RELATIVISTIC PLASMA EMISSION AND PULSAR RADIO EMISSION: A CRITIQUE

D. B. MELROSE¹ AND M. E. GEDALIN,²

Received 1998 November 29; accepted 1999 March 17

ABSTRACT

Relativistic plasma emission due to a beam instability in the polar cap regions is examined critically as a pulsar radio emission mechanism. Wave dispersion in the pulsar plasma is discussed, based on the use of a relativistic plasma dispersion function. The growth rate for the beam instability is estimated in the rest frame of the plasma for parallel Langmuir waves, L-O mode waves, and oblique Alfvén waves. The first two of these imply frequencies that are much higher than the observed frequencies for plausible parameters, suggesting that they are not viable as pulsar radio emission mechanisms. Growth of Alfvén waves requires that the beam speed equal the phase speed of the Alfvén waves, and this condition cannot be satisfied within the light cylinder, except for an extremely high energy beam. It is suggested that either the plasma parameters in the source region are quite different from what is currently considered plausible or the emission mechanism does not involve a beam instability. Alternative pulsar radio emission mechanisms should be explored further.

Subject headings: plasmas — pulsars: general — radio continuum: stars — relativity

1. INTRODUCTION

In polar-cap models for pulsars (e.g., Ruderman & Sutherland 1975; Arons 1983) the source region for the radio emission is assumed to be populated by a *pulsar plasma*, which is defined as an intrinsically extremely relativistic, streaming, one-dimensional, strongly magnetized, electron-positron pair plasma. However, the radio emission mechanism is still not adequately understood. Perhaps the most widely favored mechanism involves a beam instability in which the free energy associated with some relative streaming motion between different particle distributions in the outflowing pair plasma is transferred to waves in the plasma, with these waves producing the escaping radiation either directly or indirectly. Here this mechanism is referred to as relativistic plasma emission (RPE), based on the analogy with plasma emission in solar radio bursts, in which a beam of nonrelativistic electrons generates Langmuir waves, which produce transverse waves at the fundamental or second harmonic of the plasma frequency, ω_p . RPE was first discussed by Ginzburg, Zheleznyakov, & Zaitsev (1969), who noted the analogy with solar radio emission, and there is now extensive literature on various forms of RPE (e.g., Tsytovich & Kaplan 1972; Kaplan & Tsytovich 1973; Suvorov & Chugunov 1973, 1975; Hinata 1976a, 1976b; Hardee & Rose 1976, 1978; Benford & Buschauer 1977; Lominadze, Mikhailovskii, & Sagdeev 1979; Asséo, Pellat, & Sol 1983; Egorenkov, Lominadze, & Mamramdze 1983; Lyubarskii 1992, 1993; Asséo 1993, 1995; Weatherall 1994; Asséo & Melikidze 1998). In other early literature on pulsar radio emission, curvature emission by bunches was favored as the emission mechanism (e.g., Ruderman & Sutherland 1975), but this is no longer considered viable (Melrose 1981). Besides versions of RPE, several different pulsar radio emission mechanisms remain under consideration, including maser curvature emission (e.g., Zheleznyakov & Shaposhnikov 1979; Shaposhnikov 1981; Larroche & Pellat 1987; Chugunov & Shaposhnikov

1988; Luo & Melrose 1992, 1995), variants of free electron maser emission such as linear acceleration emission or Raman scattering (e.g., Melrose 1978; Kroll & McMullin 1979; Rowe 1992, 1995), an instability associated with curvature drift motions (e.g., Kazbegi, Machabeli, & Melikidze 1987; Luo, Melrose, & Machabeli 1994), and an anomalous Doppler instability (e.g., Lominadze, Machabeli, & Usov 1983; Machabeli & Usov 1989; Kazbegi et al. 1991).

In the present paper the application of RPE to pulsars is discussed critically. This investigation was motivated in part by the suggestion by Kunzl et al. (1998) that the frequency of Langmuir waves in a pulsar magnetosphere is too high for RPE to be compatible with the observed frequencies of pulsar radio emission. Kunzl et al. (1998) used an oversimplified model for the dispersion of these waves (Allen & Melrose 1982), and their argument needs to be reconsidered based on a more realistic and a more detailed treatment of the wave properties and of the processes by which these waves produce escaping radiation. A suggested alternative form of RPE is the growth of Alfvén waves rather than Langmuir waves (Tsytovich & Kaplan 1972). Alfvén waves can grow only if the resonance condition, that the beam speed equal the phase speed of the waves, is satisfied, and this proves very restrictive, as shown below, being satisfied only under exceptional circumstances. These difficulties lead to serious doubts as to whether RPE is viable as a pulsar radio emission mechanism.

An essential ingredient in a detailed discussion of RPE is a treatment of the properties of the waves in the source region of the radio emission, which is assumed to be the polar-cap regions. The pulsar plasma in these regions is thought to be generated in a multistage process (e.g., Sturrock 1971; Ruderman & Sutherland 1975; Arons 1983): a vacuum electric field accelerates primary particles to very high energies, these emit gamma rays nearly along B , and the gamma rays subsequently decay into secondary pairs in a pair production front (PPF). The number density of the primary particles is of order the Goldreich-Julian value, n_{GJ} , and the number density of the secondary particles is greater than this by a multiplicity factor, M , which is thought to be large but is poorly determined (e.g., Shibata, Miyazaki, & Takahara 1998). The secondary particles are extremely rela-

¹ Research Centre for Theoretical Astrophysics, School of Physics, University of Sydney, Australia.

² Department of Physics, Ben Gurion University of the Negev, Israel.

tivistic, with energy of order $1/M$ times that of the primary particles in simple models. The secondary particles rapidly radiate away any perpendicular (to \mathbf{B}) energy due to gyro-magnetic emission, so that the particle motions are one-dimensional along \mathbf{B} . The secondary plasma is expected to be intrinsically extremely relativistic in the sense that the mean energy spread is a substantial fraction of the bulk streaming energy, so that the particle distributions remain extremely relativistic even when described in the rest frame of the plasma.

There is now extensive literature on the wave properties in a pulsar plasma (e.g., Tsytovich & Kaplan 1972; Suvorov & Chugunov 1973, 1975; Godfrey, Shanahan, & Thode 1975; Melrose & Stoneham 1977; Gedalin & Machabeli 1983; Volokitin, Krasnoselskikh, & Machabeli 1985; Arons & Barnard 1986; Beskin, Gurevich, & Istomin 1988; Lyutikov 1998). It is known that there are three natural wave modes, which are given a confusing variety of names, usually based on an analogy with a nonrelativistic plasma. The names used here are as follows: The magnetoacoustic (or X or t) mode is the strictly transverse with an electric vector orthogonal to both \mathbf{B} and to the wave vector, \mathbf{k} . The other two modes are neither strictly transverse nor strictly longitudinal, except in special cases. One important special case is for parallel (to \mathbf{B}) propagation when they are the parallel Langmuir mode, which is longitudinal, and the parallel Alfvén-O mode, which is transverse. For oblique propagation these two modes reconnect into the Alfvén mode and the L-O mode.

Many of the important features of wave dispersion in a pulsar plasma can be treated in terms of appropriate moments of the particle distribution (e.g., Lominadze & Mikhailovskii 1979; Lominadze et al. 1979; Volokitin et al. 1985). However, a more thorough treatment requires the introduction of a relativistic plasma dispersion function (RPDF), which depends explicitly on the form of the distribution function. This approach was followed by Arons & Barnard (1986), who chose a “water bag” distribution. However, this distribution function is discontinuous, and to describe the wave properties adequately it is necessary to choose a distribution function with continuous first and second derivatives (Gedalin, Melrose, & Gruman 1998, hereafter GMG). Melrose et al. (1999, hereafter MGKF) investigated several different distribution functions and found that the wave dispersion is not particularly sensitive to the choice in the extremely relativistic limit. The distribution function chosen here for most illustrative purposes is a Jüttner (relativistic thermal) distribution.

Several forms of beam instability have been suggested for RPE. Two forms considered in the earlier literature are the primary particles flowing through the secondary particles (e.g., Hardee & Rose 1976) and the relative motions of electrons to positrons associated with a required net current (Cheng & Ruderman 1977), but it was argued that neither of these can lead to adequate growth (e.g., Benford & Buschauer 1977; Asséo, Pellat, & Rosado 1980). A widely favored suggestion is to appeal to the production of the secondary pairs being nonuniform in space and time, resulting in bursts of plasma production; then localized bursts of escaping plasma can lead to an instability when the faster particles in a trailing bunch overtake the slower particles in a preceding bunch (Usov 1987; Usov & Usov 1988; Asséo & Melikidze 1998). Recent investigations suggest that a steady state model for the PPF is unrealistic

(e.g., Shibata et al. 1998; Harding & Muslimov 1998), and it seems plausible that the generation of the secondary pairs is highly structured in space and time, as required by this suggestion for a beam instability to be effective. Another suggestion is that a return flux of particles of one sign is needed to satisfy continuity of the current (Lyubarskii 1992), resulting in counterstreaming motions.

In § 2 the assumptions concerning the plasma properties are summarized, and the properties of low-frequency waves, concentrating on the subluminal region of relevance to RPE, are described. In § 3 the growth rates for the various waves due to a beam instability are estimated, and the escape of the radiation is discussed. All the detailed analysis is carried out in the plasma rest frame, and in § 4 the results are transformed to the pulsar frame, which is not distinguished from the laboratory frame. In § 5 the implications of the various restrictions on RPE are compared with observational constraints, and the results are discussed in § 6. Units with $c = 1$ are used throughout.

2. WAVE DISPERSION IN THE PLASMA REST FRAME

In this section the properties of low-frequency waves in a pulsar plasma are described choosing the rest frame of the plasma.

2.1. The Model for the Plasma

In describing the plasma in the pulsar magnetosphere the following assumptions are made: For the *strong field limit*, an expansion is made in inverse powers of the magnetospheric magnetic field, B , with terms up to second order retained. For the *one-dimensional distribution*, the particles are assumed to be all in their lowest Landau orbital, corresponding classically to zero gyroradius. For the *extremely relativistic limit*, the particles are assumed to be intrinsically extremely relativistic, in the sense that in the rest frame of the plasma, the spread in particle energies is much greater than their rest energy. For *weak inhomogeneity*, gradients in the plasma parameters and curvature of the field lines are ignored, and plane wave solutions are sought. For the *low-frequency, long-wavelength limit*, the waves are assumed to be of low frequency and long wavelength, in the sense that their frequency, ω , and wavenumber, k , are much less than the cyclotron frequency of the particles. For *weak gyro-tropy*, an expansion is made in inverse powers of the multiplicity factor M for the secondary pairs, and the gyro-tropic terms, which are first order in $1/M$, are ignored.

2.2. The Plasma Rest Frame

It is convenient to treat the waves dispersion in the rest frame of the plasma. In this frame, let the distribution function of the particles be $f(u)$, where $u = p/m$ is the 4-speed of the particles. Averages over any function $K(u)$ of u are described by angular brackets:

$$\langle K \rangle = \int_{-\infty}^{\infty} du K(u) f(u), \quad \int_{-\infty}^{\infty} du f(u) = 1. \quad (1)$$

The assumption that the plasma is intrinsically relativistic corresponds to $\langle \gamma \rangle \gg 1$, with $\gamma = (1 + u^2)^{1/2}$. The speed of the particle is $v = u/\gamma$.

Let the electrons and positrons have number densities n_{\pm} . The total number density $n = n_{+} + n_{-}$ and the mean

Lorentz factor $\langle\gamma\rangle$ are incorporated into the definitions,

$$\omega_p = \left(\frac{e^2 n}{\epsilon_0 m} \right)^{1/2}, \quad v_A = \langle\gamma\rangle^{-1/2} \frac{\Omega_e}{\omega_p}, \quad (2)$$

of the plasma frequency and the Alfvén speed, respectively, with $\Omega_e = eB/m$. Another parameter that appears below is the mean square speed, \tilde{v}^2 , defined by writing

$$\langle\gamma v^2\rangle = \langle\gamma\rangle \tilde{v}^2. \quad (3)$$

In an extremely relativistic plasma one has $\tilde{v}^2 \approx 1$.

By definition, in the plasma rest frame one has $n_+ v_+ + n_- v_- = 0$, where v_{\pm} are the bulk velocities of the electrons and positrons. In a corotating pulsar magnetosphere one has $n_+ \neq n_-$, because the charge density $-e(n_+ - n_-) = en_{GJ}$ and the current density $J = -e(n_+ v_+ - n_- v_-) \sim en_{GJ}$ are nonzero, where

$$n_{GJ} = -\frac{2\epsilon_0 \Omega_r B \cos \chi}{e} \quad (4)$$

is the Goldreich-Julian density, with Ω_r the angular speed of rotation of the neutron star and χ the angle between the magnetic and rotation axes. Provided that the multiplicity, M , is large, one has $n_+ \approx n_- = Mn_{GJ}$, so that in the rest frame, the difference in number densities, $n_+ - n_-$, and in the bulk velocities, $v_+ - v_-$, are of order $1/M$ and can be neglected to a first approximation in an expansion in $1/M$. This corresponds to neglecting any gyrotropy, so that the modes have no circular or elliptical polarization.

2.3. The RPDF

The RPDF used here (see MGKF) is defined by

$$W(z) = \int_{-\infty}^{\infty} \frac{du}{z-v} \frac{df(u)}{du} = \int_{-1}^1 \frac{dv}{z-v} \frac{df(v)}{dv} = \left\langle \frac{1}{\gamma^3(z-v)^2} \right\rangle, \quad (5)$$

where a partial integration is performed in the final form and the definition in equation (1) is used. Different intrinsically relativistic distribution functions have been chosen in the literature, including exponential, $f(u) \propto \exp(-u^2/2u_m^2)$ (Lominadze & Mikhailovskii 1979), power-law (Suvorov & Chugunov 1975), and water bag (Arons & Barnard 1986) distributions. GMG considered hard-bell and soft-bell distributions, which are of the form $f(u) \propto (u_m^2 - u^2)^n$ for $u^2 < u_m^2$ with $f(u) = 0$ for $u^2 > u_m^2$, and GMG also considered a one-dimensional Jüttner distribution. MGKF explored the

properties of the RPDF in detail and found that its important features are not particularly sensitive to the choice of $f(u)$ for a given $\langle\gamma\rangle$. In this paper our detailed results are all for a Jüttner distribution,

$$f(u) = \frac{e^{-\rho\gamma}}{2K_1(\rho)}, \quad (6)$$

where $\rho = m/T$ is the inverse of the temperature in units of the rest mass and $K_\nu(\rho)$ is a Macdonald function (a modified Bessel function). In this case the various averages may be evaluated explicitly. Some specific averages are given in Table 1 along with approximate values in the extremely relativistic limit $\rho \ll 1$. In particular, one has $\langle\gamma\rangle \approx 1/\rho$, $\tilde{v}^2 \approx 1 - \rho^2 \ln(2/\rho)$, and $\langle\gamma^{-3}\rangle \approx \rho$, for $\rho \ll 1$. The RPDF (5) for the Jüttner distribution (6) is related to the function defined by Godfrey, Newberger, & Taggart (1975),

$$T(z, \rho) = \int_{-1}^1 dv \frac{e^{-\rho\gamma}}{v-z}, \quad (7)$$

with the relation being

$$z^2 W(z) = \frac{z^2 T'(z, \rho)}{2K_1(\rho)}. \quad (8)$$

The imaginary part of this RPDF is

$$\frac{z^2 \text{Im}[T'(z, \rho)]}{2K_1(\rho)} = \frac{\pi \rho \gamma_0^3 z^3}{2K_1(\rho)} \exp(-\rho\gamma_0), \quad (9)$$

with $\gamma_0 = (1 - z^2)^{-1/2}$, implying that Landau damping is weak but not strictly zero for $1/\rho \ll \gamma_0 < \infty$ and strictly zero for superluminal waves ($z > 1$).

Figure 1 illustrates the changes in the RPDF as one passes from the nonrelativistic to the mildly relativistic regime. There is a single peak in the RPDF, with the peak occurring at a phase speed, z , of order the thermal speed and with a height that increases with the mean thermal energy. The asymptotic limit ($z \rightarrow \infty$), which is unity in the nonrelativistic limit, decreases as the plasma becomes increasingly relativistic. These effects become more extreme as the particles become extremely relativistic, as shown in Figure 2, where the RPDF is plotted in a different way to illustrate these properties. Important details in Figure 2 are the asymptotic value, which determines the relativistic plasma frequency, the value at $z = 1$, which determines the minimum frequency of subluminal Langmuir waves, and the peak value, which determines the maximum frequency of parallel Langmuir waves.

TABLE 1
RELEVANT AVERAGES OVER THE JÜTTNER DISTRIBUTION

Average	Exact Value	Value for $\rho \ll 1$
$\langle\gamma\rangle$	$\frac{K_2(\rho) + K_0(\rho)}{2K_1(\rho)}$	$\frac{1}{\rho}$
$\langle\gamma^n\rangle$	$\frac{K_{n+1}(\rho)}{2^n K_1(\rho)} + \sum_{i=1}^n \frac{(n+2-i)K_{n-i}(\rho)}{2^n K_1(\rho)}$	$\frac{n!}{\rho^n}$
$\langle\gamma^{-1}\rangle$	$\frac{K_0(\rho)}{K_1(\rho)}$	$\rho[\ln(2/\rho) - 0.577 \dots]$
$\langle\gamma^{-(n+1)}\rangle$	$\frac{K_n(\rho)}{K_1(\rho)}$	$\frac{\sqrt{\pi}\Gamma(n/2)}{2\Gamma(n/2 + 1/2)} \rho$

NOTE.—Averages are given exactly and in the extremely relativistic limit $\rho \ll 1$.

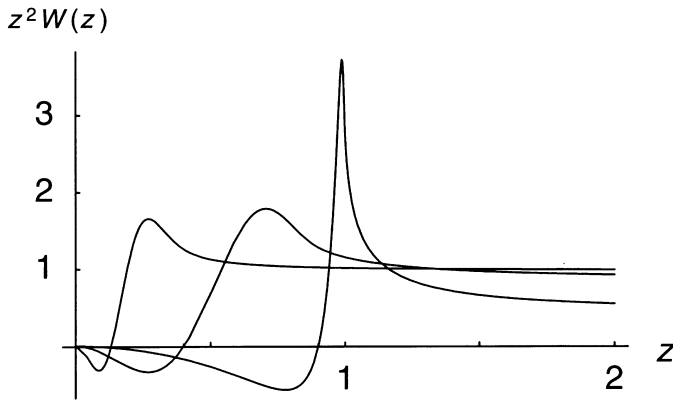


FIG. 1.—RPDF $z^2 W(z)$ plotted as a function of phase speed z for three Jüttner distributions: $\rho = 100$ (left curve), $\rho = 10$ (center curve), and $\rho = 1$ (right curve).

2.4. The Wave Properties

Following MGKF, on writing the wave equation in the form $\Lambda_{ij} e_j = 0$, where e is the polarization vector (which is a unimodular vector along the electric vector of the wave), one has

$$\begin{aligned}\Lambda_{11} &= a - \frac{b}{z^2}, \quad \Lambda_{22} = a - \frac{b - \sin^2 \theta}{z^2}, \\ \Lambda_{13} &= \Lambda_{31} = \frac{b}{z^2} \tan \theta, \\ \Lambda_{33} &= 1 - \frac{\omega_p^2}{\omega^2} z^2 W(z) - \frac{b}{z^2} \tan^2 \theta, \\ a &= 1 + \frac{1}{v_A^2}, \quad b = 1 - \frac{\tilde{v}^2}{v_A^2}.\end{aligned}\quad (10)$$

The dispersion equation factorizes into the following two equations:

$$\Lambda_{22} = 0, \quad (11)$$

$$\Lambda_{11} \Lambda_{33} - \Lambda_{13}^2 = 0. \quad (12)$$

Equation (11) gives the dispersion relation for the magnetoacoustic (or X or t) mode, and equation (12) is the dispersion equation for the L-O mode and the Alfvén mode. The

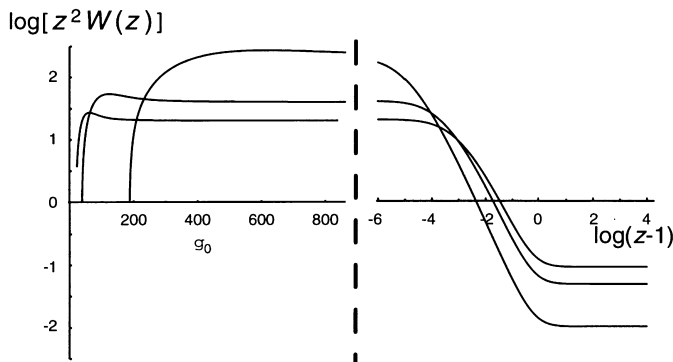


FIG. 2.—RPDF $z^2 W(z)$ plotted for three Jüttner distributions in the relativistic regime: $\rho = 0.1$ (left curve), 0.05 (center curve), and 0.01 (right curve). In order to show the extremely large peak just below $z = 1$, the logarithm of $z^2 W(z)$ is plotted as a function of $\gamma_0 = 1/(1 - z^2)^{1/2}$ for $z < 1$ and as a function of $\log(z - 1)$ for $z > 1$.

polarization vector for the magnetoacoustic mode is along the 2-axis, and the polarization vector for the other two modes is in the 1-3 plane, with

$$\frac{e_1}{e_3} = -\frac{\Lambda_{33}}{\Lambda_{13}} = -\frac{\Lambda_{13}}{\Lambda_{11}}, \quad (13)$$

which are to be evaluated at the appropriate solution of the dispersion equation (12).

2.5. The Magnetoacoustic Mode

The dispersion relation for the magnetoacoustic mode follows from equation (11). Solving for the frequency and for the phase velocity gives

$$\begin{aligned}\omega_t(k, \theta) &= k \left(\frac{v_A^2 - \tilde{v}^2 \cos^2 \theta}{v_A^2 + 1} \right)^{1/2}, \\ z = z_t &= \left(\frac{b - \sin^2 \theta}{a} \right)^{1/2},\end{aligned}\quad (14)$$

respectively. There can be no Landau damping for magnetoacoustic waves, because the polarization is along the 2-axis and so does not couple to the parallel currents associated with the motion of the particles along the field lines. For the same reason, the magnetoacoustic mode cannot be generated in a beam instability in which the beam is parallel to \mathbf{B} .

2.6. The Parallel Langmuir and Alfvén Modes

The waves of interest here are in the two branches of the solution of the dispersion equation (12). For parallel propagation ($\theta = 0$) this factorizes into a dispersion equation, $\Lambda_{33} = 0$, for the parallel Langmuir waves and a dispersion equation for the parallel Alfvén-O mode, $\Lambda_{11} = 0$. For these parallel modes the polarization vectors are along the 3-axis (longitudinal polarization) and the 1-axis, respectively. The dispersion relations are plotted in Figure 3 for a mildly relativistic plasma and in Figure 4 for an extremely relativistic plasma.

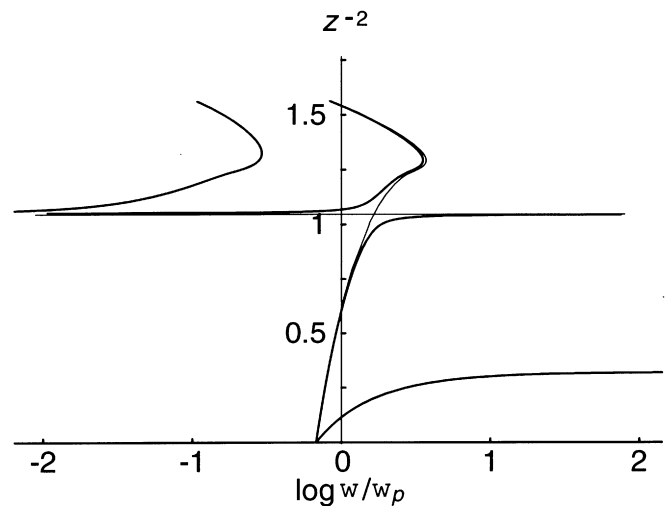


FIG. 3.—Dispersion curves for a mildly relativistic plasma with a distribution function $f(u) \propto (u_m^2 - u^2)^3$, $u_m = v_m/(1 - v_m^2)^{1/2}$, $v_m = 0.9$, and $z_A = 0.95$, and for three angles: $\theta = 0$ (thin curves), $\theta = 0.1$ (inner solid curves), and $\theta = 1$ (outer solid curves). For $\theta = 0$, the Langmuir mode is the rising curve, and the Alfvén mode is the horizontal line. For $\theta \neq 0$, the L-O mode is the branch of the curve to the lower right, and the Alfvén mode is the branch of the curve to the upper left.

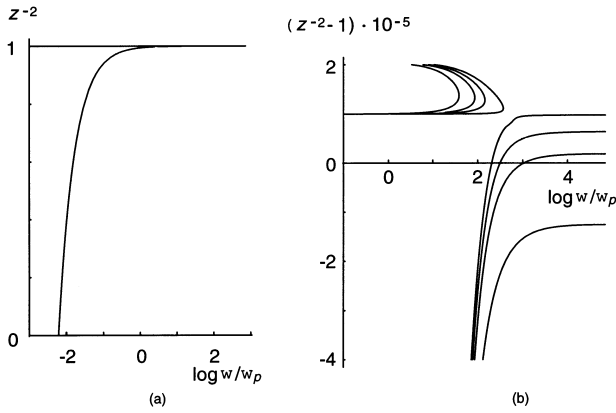


FIG. 4.—Dispersion curves analogous to those in Fig. 3 for an extremely relativistic plasma, $\langle\gamma\rangle = 100$ and $1 - z_A = 10^{-5}$. (a) The Langmuir mode is the rising curve, and the Alfvén mode is indistinguishable from a horizontal line at $z = 1$. (b) The panel is on a different scale for $\theta = 0.5 \times 10^{-3}$ (innermost curves), 1×10^{-3} , 2×10^{-3} , and 5×10^{-3} (outermost curves).

The dispersion relation for the parallel Langmuir mode is

$$\omega = \omega_L(z) = \omega_p [z^2 W(z)]^{1/2}, \quad z = z_L = \frac{\omega_L(z)}{k_{\parallel}}. \quad (15)$$

There is a minimum frequency of Langmuir waves corresponding to the cutoff ($k \rightarrow 0$ for nonzero ω) at the frequency ω_c , given by

$$\omega_c = \omega_p [z^2 W(z)]_{z=\infty}^{1/2} = \omega_p \langle\gamma^{-3}\rangle^{1/2}, \quad (16)$$

which is conventionally identified as the *relativistic plasma frequency*. For any extremely relativistic plasma, $\langle\gamma^{-3}\rangle$ is of order $1/\langle\gamma\rangle$ in an expansion in powers of $1/\langle\gamma\rangle$ (see Table 1). As in a nonrelativistic thermal plasma, the frequency of the Langmuir waves increases with increasing k (decreasing z). Their frequency at $z = 1$ is denoted ω_1 , given by

$$\omega_1^2 = \omega_p^2 W(1) = \omega_p^2 \langle\gamma\rangle (1 + \tilde{v}^2), \quad (17)$$

above which the parallel Langmuir waves are subluminal. It follows that in an extremely relativistic plasma, the frequency ratio, ω_1/ω_c , is large ($\sim \langle\gamma\rangle$; e.g., Lominadze et al. 1979). For slightly subluminal Langmuir waves one may expand in powers of $1 - z = 1/2\gamma_0^2 + \dots$, and to first order equation (15) gives

$$\begin{aligned} \omega_L^2(z) &= \omega_p^2 [\langle\gamma^{-3}(1 - v)^{-2}\rangle + 2(1 - z) \\ &\quad \times \langle\gamma^{-3}(1 - v)^{-2}\rangle + \dots] \\ &= \omega_p^2 2\langle\gamma\rangle [1 + 2\langle\gamma^3\rangle/\langle\gamma\rangle\gamma_0^2 + \dots], \end{aligned} \quad (18)$$

where the final expansion is in powers of both $1/\langle\gamma\rangle$ and $1/\gamma_0$.

Although the parallel Langmuir mode extends into the subluminal range $z < 1$, it extends only for a narrow range of phase speeds $z_{\text{peak}} \lesssim z < 1$, where z_{peak} is the phase speed at which $z^2 W(z)$ has its peak value. Landau damping becomes strong at $z \lesssim z_{\text{peak}}$ (see Fig. 1 and MGKF).

The other factor in the dispersion equation (12) for parallel propagation gives $\Lambda_{11} = 0$, which gives the dispersion relation for the Alfvén-O mode:

$$z = z_A, \quad z_A = \left(\frac{b}{a}\right)^{1/2} = \left(\frac{v_A^2 - \tilde{v}^2}{1 + v_A^2}\right)^{1/2}. \quad (19)$$

This dispersion relation is the same as for the magnetoacoustic mode for parallel propagation (see eq. [14]). The electric vector for parallel Alfvén-O mode waves is along the 1-axis, so there is no Landau damping for the same reason as for the magnetoacoustic mode.

2.7. Oblique Waves

The dispersion relation (12) may be written in the form

$$\frac{\omega^2}{\omega_p^2} = \frac{z^2 W(z)(z^2 - z_A^2)}{z^2 - z_B^2} \quad (20)$$

(MGKF), with $z_A^2 = b/a$ and $z_B^2 = z_A^2 + b \tan^2 \theta$. In the limit of parallel propagation one has $z_B \rightarrow z_A$, and equation (20) reproduces the dispersion relation (15) for parallel Langmuir waves for $z \neq z_A$, with the dispersion relation for parallel Alfvén-O mode. For $z_A > z_0$ these two dispersion curves intersect, defining a crossover frequency ω_{co} ,

$$\omega_{co} = \omega_p [z_A^2 W(z_A)]^{1/2}, \quad (21)$$

and a corresponding wavenumber $k_{\parallel} = \omega_{co}/z$. As pointed out in earlier literature (e.g., Hardee & Rose 1976; Arons & Barnard 1986) and as illustrated in Figure 3, for slightly oblique propagation the dispersion curves reconnect near this intersection point and then deviate away from each other with increasing θ . The higher frequency reconnected mode is the L-O mode, and in the limit $\theta \rightarrow 0$ it reduces to the Alfvén-O mode for $\omega > \omega_{co}$ and to the Langmuir mode for $\omega < \omega_{co}$. The lower frequency branch is the Alfvén mode, and in the limit $\theta \rightarrow 0$ it reduces to the Langmuir mode for $\omega > \omega_{co}$ and to the Alfvén-O mode for $\omega < \omega_{co}$.

The expressions in equation (13) for the polarization vector may be rewritten in the notation used in equation (20). Two forms are

$$\frac{e_1}{e_3} = - \frac{z^2 [1 - \omega_L^2(z)/\omega^2] - b \tan^2 \theta}{b \tan \theta} = - \frac{z_A^2 \tan \theta}{z^2 - z_A^2}, \quad (22)$$

with $\omega_L(z)$ the frequency (15) of parallel Langmuir waves.

2.8. The L-O Mode

The L-O mode exists only for $z > z_B$. The lowest frequency L-O mode waves are near the Langmuir cutoff at $\omega = \omega_c$ (see eq. [16]), which is independent of θ in the limit $z \rightarrow \infty$. Equation (20) implies that the cutoff frequency is given by equation (16) independent of θ . The final form of equation (22) shows that near the cutoff, one has $e_1/e_3 \rightarrow 0$, so that the polarization is along \mathbf{B} , which is longitudinal only for parallel propagation. The highest frequency L-O mode waves correspond to $z^2 \rightarrow z_B^2$ in equation (20). The polarization of these waves is given by $e_1/e_3 \rightarrow -1/a \tan \theta$, which is a transverse polarization in the approximation $a \approx 1$. Specifically, the longitudinal part of the polarization is $\sin \theta \cos \theta/v_A^2 \ll 1$.

Most of the interest here is in the subluminal L-O mode waves. The waves can be subluminal only for $z_B < 1$, and such waves exist only above a minimum frequency, $\omega_1(\theta)$, and at angles of propagation less than a maximum, θ_{max} . The frequency above which the L-O mode is subluminal is

given by

$$\omega_1^2(\theta) = \omega_p^2 W(1) \frac{(1 - z_A^2)}{1 - z_B^2} \approx \omega_p^2 \langle \gamma \rangle (1 + \tilde{v}^2) \left(1 - \frac{v_A^2 \theta^2}{1 + \tilde{v}^2}\right)^{-1}, \quad (23)$$

where $v_A^2 \gg 1$ is assumed in the approximate form. The region of subluminal waves moves to higher frequencies with increasing θ and disappears above a maximum angle, $\theta = \theta_{\max}$, given by

$$\theta_{\max} \approx \left(\frac{1 + \tilde{v}^2}{v_A^2} \right)^{1/2}, \quad (24)$$

for $v_A^2 \gg 1$. The polarization is nearly transverse for $\omega \gg \omega_{co}$, with $e_1 \approx 1$ and $e_3 \approx \theta$ for $\theta \ll 1$. For $\omega \approx \omega_{co}$ the polarization may be approximated by

$$\frac{e_1}{e_3} \approx -\frac{1 - \omega_L^2(z)/\omega^2 - \theta^2}{\theta}. \quad (25)$$

The waves become increasingly longitudinally polarized, $e_1/e_3 \rightarrow 0$, in the limit $\omega \rightarrow \omega_L(z)$ and $\theta \rightarrow 0$, corresponding to the parallel Langmuir mode.

2.9. Alfvén Mode

The lower frequency reconnected mode is the oblique Alfvén mode, and its dispersion relation follows directly from equation (20), as discussed by GMG and MGKF. In contrast to the L-O mode, the dispersion curve for the oblique Alfvén mode deviates to lower frequencies and lower phase speeds with increasing θ . For $\omega^2 \ll \omega_{co}^2$, equation (20) gives

$$z^2 \approx z_A^2 - \frac{\omega^2}{\omega_{co}^2} \theta^2, \quad (26)$$

and the polarization may be approximated by equation (25). This polarization is nearly along the 1-axis:

$$\frac{e_1}{e_3} \approx \frac{\omega_L^2(z)}{\omega^2 \theta}. \quad (27)$$

3. RELATIVISTIC PLASMA EMISSION

In this section, analytic approximations for beam instabilities in a pulsar plasma are summarized, and how the resulting wave turbulence produces escaping radiation is briefly discussed.

3.1. Kinetic and Reactive (Hydrodynamic) Beam Instabilities

In the class of models of interest here, there is a background plasma through which a higher energy, lower density beam propagates. The background plasma determines the properties of the waves, and the beam determines the wave growth. The beam is assumed to have a speed $v_b = (\gamma_b^2 - 1)^{1/2}/\gamma_b$ (where γ_b is its Lorentz factor), a spread $\Delta\gamma_b$ in Lorentz factors, a number density n_b , and a distribution function $f_b(u)$.

The spread $\Delta\gamma_b$ in Lorentz factors depends on the model. For a beam of primary particles, the spread is expected to

be small because of the fact that all the particles are accelerated by the same parallel electric field. A beam of secondary particles, perhaps propagating through a plasma dominated by tertiary particles, may be quite broad. Here we simply assume that $\Delta\gamma_b$ is sufficiently small that the beam particles do not overlap significantly with the background particles.

Wave growth can occur in two limiting cases: a *kinetic* instability, in which the growth rate is smaller than the intrinsic bandwidth of the growing waves, and a *reactive* instability (also called a *hydrodynamic* instability), in which this inequality is reversed (e.g., Egorenkov et al. 1983 and the review by Lominadze et al. 1986). Provided that these inequalities are strong ones the two limiting cases may be treated separately. The beam appears in the dispersion equation through a correction from $\delta\Lambda_{33}$ to Λ_{33} , with the imaginary and real parts of $\delta\Lambda_{33}$ being relevant for the kinetic and reactive instabilities, respectively.

A kinetic instability is treated as negative absorption, which involves the imaginary part of $\text{Im } W_b(z)$ because of the beam, with

$$\begin{aligned} \text{Im } \delta\Lambda_{33} &= -\frac{\omega_p^2}{\omega^2} z^2 \text{Im } W_b(z) \\ &= -\frac{\omega_p^2}{\omega^2} z^2 \pi \frac{n_b}{n} \gamma_0^3 \left[\frac{df_b(u)}{du} \right]_{u=\gamma_0 z}. \end{aligned} \quad (28)$$

The reactive instability is treated by including the contribution of the real part of $W_b(z)$ to the dielectric tensor and neglecting the spread in Lorentz factors in the beam:

$$\text{Re } \delta\Lambda_{33} = -\frac{\omega_p^2}{\omega^2} z^2 \text{Re } W_b(z) = -\frac{\omega_p^2}{\omega^2} \frac{n_b}{n} \frac{z^2}{\gamma_b^3 (z - v_b)^2}. \quad (29)$$

A reactive instability then occurs when the dispersion equation has complex solutions, with the growth rate identified as the imaginary part of the growing solution.

3.2. Growth of Parallel Langmuir Waves

A beam propagating along \mathbf{B} implies a current along \mathbf{B} , and this couples to any wave that has an electric vector with a component along \mathbf{B} . Parallel Langmuir waves have their electric field along \mathbf{B} , but magnetoacoustic and parallel Alfvén-O modes have their electric vector orthogonal to \mathbf{B} . Hence, for parallel propagation, only Langmuir waves grow because of a beam instability.

In the case of the kinetic instability, we neglect the beam contribution into the real part of Λ_{33} , retaining only the imaginary part. The dispersion equation becomes

$$1 - \frac{\omega_p^2}{k_{\parallel}^2} W(z) - i\pi \frac{\omega_p^2}{k_{\parallel}^2} \left(\frac{n_b}{n} \right) \frac{\gamma_b^3}{(\Delta\gamma_b)^2} = 0, \quad (30)$$

where it is implicit that $z = \omega/k_{\parallel}$ has a small imaginary part corresponding to wave damping or growth. Ignoring the imaginary terms, equation (30) reproduces the dispersion relation (15), and the imaginary terms are evaluated at this dispersion relation in order to find the absorption coefficient or growth rate. In estimating the final term in equation (30), we assume that $z = v_b$ corresponds to the maximum growth rate (approximately the maximum slope of the beam

distribution function) and that $\Delta\gamma_b$ is the effective width of the beam, and we make the approximations $f \sim 1/\Delta\gamma_b$ and $df/du \sim 1/(\Delta\gamma_b)^2$.

From the foregoing analysis of the wave dispersion, at the resonance one has $k_{\parallel} \sim \omega_p \langle \gamma \rangle^{1/2}$, and the growth rate, Γ , may be approximated by

$$\frac{\Gamma}{\omega} \sim \left(\frac{n_b}{n} \right) \frac{\gamma_b^3}{(\Delta\gamma_b)^2} \frac{1}{W'(z)}, \quad (31)$$

$$W'(z) = \int_{-\infty}^{\infty} \frac{du}{(z-v)^2} \frac{df}{du} \sim \langle \gamma^3 \rangle \sim \langle \gamma \rangle^3. \quad (32)$$

Assuming comparable energy density in the beam and plasma background, $n\langle \gamma \rangle \sim n_b \gamma_b$, one finds

$$\frac{\Gamma}{\omega} \sim \left(\frac{\gamma_b}{\langle \gamma \rangle \Delta\gamma_b} \right)^2. \quad (33)$$

The condition for validity of the kinetic approach is $\Gamma \lesssim \Delta\omega$, where $\Delta\omega$ is the bandwidth of the excited waves, estimated to be $\Delta\omega/\omega \sim \Delta\gamma_b/\gamma_b^3$. Hence the condition for the kinetic version of the instability to apply reduces to

$$\frac{\Gamma}{\Delta\omega} \sim \left(\frac{\gamma_b}{\langle \gamma \rangle} \right)^2 \left(\frac{\gamma_b}{\Delta\gamma_b} \right)^3 \lesssim 1. \quad (34)$$

The condition (34) is never satisfied, because one always has $\gamma_b > \langle \gamma \rangle$ and $\Delta\gamma_b$. Hence the beam instability of parallel Langmuir waves can only be a reactive instability.

The reactive or hydrodynamic instability applies when the spread in velocities is unimportant and is conveniently analyzed by setting the spread to zero by assuming $f_b = \delta(v - v_b)/\gamma$. This gives a dispersion equation

$$1 - \frac{\omega_p^2}{k^2} W(z) - \frac{n_b}{n} \frac{\omega_p^2}{\gamma_b^3 (\omega - k_{\parallel} v_b)^2} = 0. \quad (35)$$

As shown by Egorenkov et al. (1983), one can distinguish two cases: the “resonant case,” in which the growth rate is of the form $\Gamma \propto (n_b/n)^{1/3}$, and the “nonresonant case,” in which the growth rate is of the form $\Gamma \propto (n_b/n)^{1/2}$. The resonant case, which has the larger growth rate, is centered on the frequency given by setting $z = v_b$ in the dispersion relation for parallel Langmuir waves, which gives $\omega_0^2 = \omega_p^2 v_b^2 W(v_b)$, and this frequency is of the same order of magnitude as for $v_b \rightarrow 1$, implying $\omega_0^2 \sim \omega_p^2 \langle \gamma \rangle$. A correction to this frequency is introduced by writing $\omega = \omega_0 + \delta\omega$ and hence $z = v_b(1 + \delta\omega/\omega)$, with $k_{\parallel} = \omega/v_b \sim \omega_0$. Substituting into equation (35) one finds

$$\left(\frac{\delta\omega}{\omega} \right)^3 \sim - \left(\frac{n_b}{n} \right) \frac{1}{\gamma_b^3 W'(v_b)}, \quad (36)$$

so that the growth rate for the reactive instability (in the resonant case) is given by

$$\frac{\Gamma}{\omega} \sim \left(\frac{n_b}{n} \right)^{1/3} \frac{1}{\gamma_b \langle \gamma \rangle}. \quad (37)$$

The results for parallel propagation remain approximately valid for waves at sufficiently small angles of propagation. The range of θ over which the waves may be assumed approximately parallel may be estimated from the expressions in equation (20) for the dispersion relation and in equation (22) for the polarization of oblique waves. Assuming $z = v_b$ for resonance with the beam, parallel approximation is approximately valid for $\theta^2 \lesssim |v_b^2 - z_A^2|$,

which requires $\theta \lesssim \min[1/v_A, 1/\gamma_b]$. For θ greater than about the minimum of $1/v_A$ and $1/\gamma_b$, the waves should be treated as L-O mode waves or oblique Alfvén waves.

3.3. Growth of Oblique Waves

In discussing growth of oblique waves, it is helpful to represent the resonance condition graphically and to compare the oblique case with the case of parallel propagation. In Figure 5 the dispersion curves are indicated schematically, in the same format as in Figures 3 and 4, with the dashed curves for parallel propagation and the solid curves for oblique propagation. The resonance condition, $z = v_b$, corresponds to a horizontal line, and two cases are illustrated, one with $v_b > z_A$ (dotted line, labeled r1 in Fig. 5) and the other with $v_b < z_A$ (dotted line, labeled r2 in Fig. 5). A resonance corresponds to the intersection of the relevant dotted line with the dispersion curve for the waves. For parallel propagation, resonance is possible for parallel Langmuir waves, as indicated in the two cases indicated by circles where these lines intersect the dispersion curve for Langmuir wave (labeled L). The dispersion curve (the line $z = z_A$) for parallel Alfvén waves is parallel to the line $z = v_b$, so that resonance is not possible, except for the special case $v_b = z_A$ when the lines coincide (which case is discussed below).

For oblique propagation, growth of L-O mode waves is possible only for $v_b > z_A$, and growth of Alfvén waves is possible only for $v_b \leq z_A$. This may be seen by inspection of the intersection of the dotted lines and solid curves in Figure 5: only line r1 can intersect the dispersion curve for L-O mode waves, and only line r2 can intersect the dispersion curve for Alfvén waves.

Resonance of the beam with L-O mode waves at high frequencies $\omega^2 \gg \omega_{co}^2$ is possible only at a specific angle for $v_b > z_A$. This follows from the dispersion relation (12) in the limit $\omega/\omega_p \rightarrow \infty$ when one has $\Lambda_{33} \approx 1 - \tan^2 \theta$, implying that high-frequency L-O mode waves have a dispersion relation $z^2 = z_A^2 + \theta^2$, where we assume $\theta^2 \ll 1$ and $a \approx 1$, $b \approx 1$ in equation (10). The resonance condition $z = v_b$

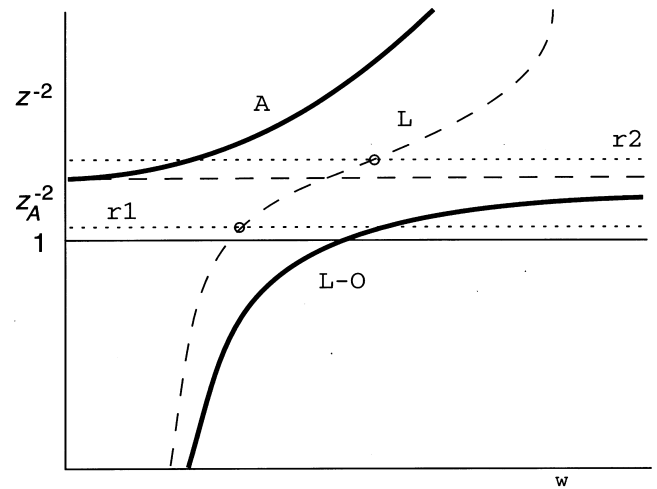


FIG. 5.—Schematic plot of dispersion curves analogous to those in Figs. 3 and 4 for a small range near the crossover frequency, ω_{co} , where the dispersion curves for the parallel Langmuir mode (dashed curve, labeled L) intersect the dispersion curves for the parallel Alfvén mode (horizontal dashed line). The thick curves indicate dispersion curves for oblique L-O mode (lower right) and Alfvén waves (upper left). The lines r1 and r2 represent resonances at $z = v_b$ with $v_b > z_A$ and $v_b < z_A$, respectively, and the circles denote the corresponding resonant parallel Langmuir waves.

determines the angle $\theta = (v_b^2 - z_A^2)^{1/2}$ at which resonance is possible. When this condition is satisfied, L-O mode waves over a broad range of frequencies can resonate with the beam particles, and hence a kinetic instability is appropriate. It follows from equation (25) that these waves have $e_3^2 \sim \theta^2$, and this factor appears in the growth rate ($n_b \rightarrow e_3^2 n_b$). As a consequence, L-O mode waves grow more slowly than do parallel Langmuir waves.

The dispersion relation for the Alfvén mode at low frequencies ($\omega^2 \ll \omega_{co}^2$) approaches $z = z_A$ independent of θ (see eq. [26]). It follows that the resonance condition $z = v_b$ is satisfied only in the special case $v_b = z_A$. In this case the spread in velocities in the beam needs to be taken into account, and the resonance can be satisfied over a broad range of frequencies so that any instability is kinetic in nature. The growth rate is evaluated by including the imaginary part of $\delta\Lambda_{33}$ (see eq. [28]) in the dispersion equation (12). This gives

$$\frac{\Gamma}{\omega} = \pi \theta^2 \frac{n_b}{n} \frac{\gamma_b^3}{\langle \gamma \rangle} \left(\frac{df}{du} \right)_{v=z_A}, \quad (38)$$

with growth corresponding to $(df_b/du)_{v=z_A} > 0$. This beam instability favors the highest frequency Alfvén waves.

In summary, wave growth is most favorable for parallel and nearly parallel Langmuir waves whose polarization is approximately longitudinal. L-O mode waves over a broad range of much higher frequencies can grow at a specific angle $\theta = (v_b^2 - z_A^2)^{1/2}$ for $v_b > z_A$. Alfvén waves over a broad range of much lower frequencies can grow, but only when the condition $v_b = z_A$ is satisfied to within the velocity spread of the beam. However, growth favors the lowest frequency for L-O mode waves and the highest frequency for Alfvén waves, so that all three cases suggest that growth of a wave with $\omega \sim \omega_p \langle \gamma \rangle^{1/2}$ is favored.

3.4. Escape of Radiation

In order to be observed as radio emission by a distant observer, the waves must be able to leave the pulsar magnetosphere. Once a wave is excited it propagates outward in the pulsar plasma, which has a gradually decreasing density and ambient magnetic field. Along the outward path the cyclotron frequency, plasma frequency, and Alfvén speed decrease. Eventually a wave encounters the cyclotron resonance, and if it has a nonzero e_1 (L-O and oblique Alfvén waves) or e_2 (magnetoacoustic waves) it experiences cyclotron damping. In the following discussion we ignore the effects of the cyclotron resonance, which will be discussed elsewhere.

Consider the effects of the inhomogeneity of the plasma on the propagation of parallel Langmuir waves as they propagate outward. Three effects need to be taken into account. First, as ω_p decreases along the ray path, the dispersion relation (15) requires that z decrease and hence that k_{\parallel} increase (with ω constant in the absence of temporal variations in the plasma parameters). In the absence of other effects, this decrease in z ultimately drives the waves into the region of phase speed where Landau damping is strong, and the waves are then absorbed by the background particles. Second, the curvature of the field lines causes the angle θ to increase (assuming that it is initially negligible). For L-O mode waves this implies an increase in phase speed, and only a modest increase is required to drive the waves into the superluminal range where they are

undamped and escape freely. Third, mode coupling needs to be taken into account in an inhomogeneous plasma. Mode coupling is effective only near a coupling point, and the only coupling point in the present theory is at $\omega = \omega_{co}$ and $\theta = 0$, where the dispersion curves for the parallel Langmuir and parallel Alfvén modes intersect. The significance of mode coupling in the present case can be understood by considering the fate of the resonant parallel Langmuir waves generated at the two resonances illustrated by circles in Figure 5. The resonance associated with line r2 occurs above the crossover frequency, and such waves move to the right along the dashed dispersion curve in Figure 5 as they propagate outward, until they encounter the region of strong Landau damping, where they are absorbed. The resonance associated with line r1 occurs below the crossover frequency, and such waves encounter the coupling point as they propagate outward. If the inhomogeneity is sufficiently weak, then even for very small θ the waves are to be regarded as L-O mode, which move to the right, on the curve L below the coupling point and on the dispersion curve $z = z_A$ above the coupling point. Hence such waves escape. Mode coupling implies that in a small range of θ about $\theta = 0$ the waves may tunnel through the coupling point and emerge on the upper right branch of the dispersion curve labeled L, so that they propagate into the region of strong Landau damping and are absorbed.

Finally, consider oblique Alfvén waves generated at $\omega \ll \omega_{co}$. As such waves propagate outward they approach the maximum frequency of the Alfvén mode (see Fig. 3), where Landau damping by the background plasma is strong. Thus, if a beam instability is effective in generating Alfvén waves, these cannot escape, and escaping radiation can result only through partial conversion of the energy flux in the Alfvén waves into either magnetoacoustic waves or L-O mode waves.

We should remark that although magnetoacoustic waves can freely escape from the pulsar magnetosphere, these waves cannot be generated by a beam instability and thus are not directly relevant to RPE.

This discussion suggests that the most favorable form of RPE is a beam instability that generates parallel Langmuir waves, which propagate outward as L-O waves and escape the magnetosphere (provided cyclotron absorption, which we ignore here, is unimportant). This free escape is possible only if the condition $v_b > z_A$ is satisfied (see the line r1 in Fig. 5).

4. TRANSFORMATION TO THE PULSAR FRAME

The analysis above is carried out in the rest frame of the plasma, where the net streaming speed of the background plasma is zero. A more relevant frame is the pulsar frame, in which the secondary pair plasma is flowing out along the field lines at a highly relativistic speed. The values of quantities in the two frames are related by a Lorentz transformation. Let the streaming speed of the outflowing plasma in the pulsar frame be v_s , with Lorentz factor $\gamma_s = 1/(1 - v_s^2)^{1/2}$. Let quantities in the pulsar frame be denoted by primes, with quantities in the plasma rest frame unprimed, as in the discussion above.

The relations between the Lorentz factors and beam velocities in the pulsar frame and the corresponding quantities in the plasma rest frame are

$$\gamma'_b = \gamma_s \gamma_b (1 + v_b v_s), \quad (39)$$

which implies $\gamma_b \approx \gamma'_b/2\gamma_s$ when all Lorentz factors are large.

The relations between the frequency, ω' , and the phase speed, z' , in the two frames are

$$\omega' = \frac{\gamma_s(z + v_s)}{z} \omega, \quad z' = \frac{z + v_s}{1 + zv_s}. \quad (40)$$

For forward-propagating waves, $z > 0$, the frequency is always higher in the pulsar frame ($\omega' > \omega$). The waves of interest here have phase speed close to the speed of light, $z \approx 1$, and then equation (40) implies $\omega' \approx 2\gamma_s \omega$ for $\gamma_s \gg 1$. The perpendicular wavenumber does not change, $k' \sin \theta' = k \sin \theta$, and this implies that in the pulsar frame, the radiation is strongly collimated into a forward cone $\sim 1/\gamma_s^2$.

The parameters $\langle \gamma \rangle$, \tilde{v}^2 , ω_p , and v_A are all defined in the rest frame, and analogous parameters can be defined in the pulsar frame. The number density in the pulsar frame is $n' = n\gamma_s$, and the magnetic field is unaffected by a Lorentz transformation along the magnetic field lines ($B' = B$). Hence on defining parameters in the pulsar frame corresponding to the plasma frequency, $\omega'_p = (e^2 n' / \epsilon_0 m)^{1/2}$, and the Alfvén speed, $v'_A = B' / (\mu_0 n' m \langle \gamma \rangle)^{1/2}$, one has

$$\omega'_p = \gamma_s^{1/2} \omega_p, \quad v'_A = \frac{v_A}{2^{1/2} \gamma_s}, \quad (41)$$

where the extremely relativistic approximation is assumed in the latter.

5. CONSTRAINTS ON RPE

In this section it is argued that for the form of RPE in which parallel Langmuir waves grow in the beam instability, the predicted frequency of emission is incompatible with the observed range of emission for pulsars. It is then argued that the essential condition $v_b = z_A$, required for Alfvén waves to grow in the beam instability, imposes a severe constraint on the allowable parameters that is not plausibly satisfied for typical pulsars.

5.1. Frequency of Langmuir Waves

Suppose that the beam instability generates parallel Langmuir waves. Then the typical frequency of the RPE that results is approximately the frequency of the Langmuir waves. This is $\sim \omega'_1$, that is, the frequency ω_1 defined by equation (17) transformed to the pulsar frame. Thus the implied emission frequency is $\omega' \approx 2\gamma_s^{1/2} \langle \gamma \rangle^{1/2} \omega'_p$. Assuming that the electron density, n' , is M times the Goldreich-Julian density, $2\epsilon_0 B/eP$, where P is the period of rotation, the numerical value of this frequency is estimated to be

$$\left(\frac{\omega'}{2\pi}\right) \sim (10 \text{ GHz}) \left(\frac{B_*}{10^{12} \text{ G}}\right)^{1/2} \left(\frac{P}{100 \text{ ms}}\right)^{-1/2} \left(\frac{r}{R_*}\right)^{-3/2} \times (M \langle \gamma \rangle \gamma_s)^{1/2}, \quad (42)$$

where the magnetic field is assumed dipolar in the sense that it varies according to $B = B_* R_*^3/r^3$ with distance r from the surface of the star ($r = R_*$). The parameters M , $\langle \gamma \rangle$, γ_s , and r/R_* are poorly constrained by existing models. In particular, estimates of r/R_* based on radius-to-frequency mapping suggest $r/R_* \sim 10$ – 10^2 , but uncertainties remain in the interpretation of the relevant data (see, e.g., recent summaries by Kramer et al. 1997 and Kijak & Gil 1998). A seemingly plausible choice of values is $M \sim 10^4$, $\langle \gamma \rangle \sim 10^2$,

$\gamma_s \sim 10^2$, and $r/R_* \sim 10^2$. Then, with $B \sim 10^{12}$ G and $P \sim 100$ ms, equation (42) gives a frequency ~ 100 GHz, which is much higher than the typical frequency of emission, ~ 1 GHz, of pulsars. Even with $M \sim 1$, $\langle \gamma \rangle \sim 10$, $\gamma_s \sim 10$, and $r/R_* \sim 10^2$, one cannot account for this typical frequency. Moreover, the peak of the radio spectrum for many pulsars is well below 1 GHz, and it is seemingly impossible to account for this in terms of equation (42).

It is concluded that RPE due to a beam instability generating parallel Langmuir waves is incompatible with the observed frequencies of pulsar radio emission for seemingly plausible parameters, as suggested by Kunzl et al. (1998). With Langmuir waves considered unacceptable on this basis, growth of L-O mode waves is similarly excluded because their frequency is higher than that of parallel Langmuir waves. According to this argument, only RPE associated with growth of Alfvén waves at $\omega' \ll \omega'_1$ would be consistent with the observed frequencies.

5.2. Requirement for Beam Resonance with Alfvén Waves

Alfvén waves at $\omega' \ll \omega'_1$ can grow only if the resonance condition $z' = v'_b$ is satisfied. Using equations (39) and (41), this condition becomes

$$\gamma'_b = 4\gamma_s^2 \frac{\Omega_e}{\omega'_1}. \quad (43)$$

On reexpressing ω'_1 as in equation (42), equation (43) becomes

$$\gamma'_b = 5 \times 10^8 \left(\frac{B_*}{10^{12} \text{ G}}\right)^{1/2} \left(\frac{P}{100 \text{ ms}}\right)^{1/2} \left(\frac{r}{R_*}\right)^{-3/2} \times \left(\frac{\gamma_s^3}{M \langle \gamma \rangle}\right)^{1/2}. \quad (44)$$

Equation (44) may be interpreted as specifying the distance, r/R_* , at which the beam instability can generate Alfvén waves:

$$\frac{r}{R_*} = 6 \times 10^5 \left(\frac{B_*}{10^{12} \text{ G}}\right)^{1/3} \left(\frac{P}{100 \text{ ms}}\right)^{1/3} \left(\frac{\gamma_s^3}{\gamma_b'^2 M \langle \gamma \rangle}\right)^{1/3}. \quad (45)$$

For plausible parameters (e.g., $M \sim 10^4$, $\gamma_s \sim 10^2$, $\langle \gamma \rangle$ somewhat smaller than γ_s , and γ'_b somewhat larger than γ_s) this distance is too large to be of relevance; specifically, it is well outside the light cylinder, where the dipole approximation used in its derivation is invalid. This conclusion applies to both normal pulsars and millisecond pulsars.

The only obvious exception that would allow the resonance to occur inside the light cylinder is if the beam energy is very high. For example, assuming that the primary particles constitute the beam and assuming $\gamma'_b \sim M\gamma_s$ and $\langle \gamma \rangle \sim \gamma_s$, the final factor in equation (45) is $\sim 1/M$, and for $M \sim 10^4$ the resonance condition is satisfied inside $r/R_* = 10^3$ for plausible parameters. However, this suggestion does not overcome another difficulty: the growth rate in equation (38) favors the maximum frequency, consistent with its derivation, and this frequency is too high ($\sim \omega_1$) to be compatible with the observations for the reasons discussed above.

6. DISCUSSION AND CONCLUSIONS

In this paper a detailed treatment of the properties of waves in polar-cap models for pulsar radio emission is

applied to a critical analysis of RPE due to a beam instability. The wave properties are derived in the rest frame of the plasma and then transformed to the pulsar frame for comparison with observations. It is well known that there are three wave modes in a pulsar plasma, and one of these, the magnetoacoustic mode (or X mode or t mode), is strictly transverse and does not couple to the beam motion. Possible beam instabilities lead to the generation of parallel Langmuir waves, oblique L-O mode waves at a much higher frequency than the parallel Langmuir waves, or oblique Alfvén waves at a much lower frequency than the parallel Langmuir waves. It is found that none of these instabilities can account for the observed radio emission for parameters that are considered plausible in polar-cap models.

The estimated frequency of RPE for parallel Langmuir waves is given by equation (42), and for plausible parameters, this frequency is much higher than the typical observed frequency of pulsar radio emission (Kunzl et al. 1998). This appears to exclude RPE due to a beam instability generating Langmuir waves. A beam instability generating L-O mode waves is excluded for the same reason. The reason that a higher frequency for emission due to this mechanism is estimated here than by most earlier authors may be summarized as follows: It is well known that Langmuir waves in a nonrelativistic plasma have frequencies just above the plasma frequency, $\omega_p = (e^2 n_e / \epsilon_0 m)^{1/2}$, and that they have a cutoff at ω_p . The corresponding cutoff frequency in a relativistic plasma is $\omega_p \langle \gamma^{-3} \rangle^{1/2}$ (see $z \rightarrow \infty$ in eq. [15], with $k \rightarrow 0$ in the final form in eq. [5]). This might suggest that in a relativistically streaming (Lorentz factor γ_s) plasma, Langmuir waves have a lower frequency, $\omega_p \gamma_s^{-3/2}$, than in the absence of relativistic effects. However, the reverse is the case. First, note that for an intrinsically relativistic plasma in its rest frame one has $\langle \gamma^{-3} \rangle \sim 1/\langle \gamma \rangle$, and the cutoff frequency is $\sim \omega_p \langle \gamma \rangle^{-1/2}$ and not $\sim \omega_p \langle \gamma \rangle^{-3/2}$. More importantly, to grow in a beam instability the Langmuir waves must be subluminal, and they are subluminal only for $\omega \gtrsim \omega_p \langle \gamma \rangle^{1/2}$. On transforming from the plasma rest frame to the pulsar frame, the frequency $\omega_1 \approx \omega_p \langle \gamma \rangle^{1/2}$ is Lorentz-boosted to the frequency $\omega'_1 \approx \omega_p 2\gamma_s \langle \gamma \rangle^{1/2}$, where ω'_p is the plasma frequency in the pulsar frame. Thus the predicted frequency of emission for this version of RPE is much higher than the plasma frequency for plausible parameters (see eq. [42]).

The foregoing discussion is based on the assumption that the beam is weak, in the sense that it does not modify the wave dispersion significantly. The referee pointed out to us that this may not be the case if the beam density is relatively high. Weatherall (1994) discussed the beam instability for two beams of comparable densities, one with a highly relativistic temperature and the other with a nonrelativistic temperature, and found maximum growth for $k = 0.29\omega_p$ for the parameters chosen. Weatherall did not plot the real part of the frequency, and presumably it is significantly modified from the weak-beam case, when $k = 0.29\omega_p$ would correspond to superluminal Langmuir waves. The implications of relaxing the weak-beam approximation need to be explored further. Our discussion assumes a weak beam with a relativistic velocity spread, whereas Weatherall's (1994) discussion applies to a stronger beam with a nonrelativistic spread.

It is concluded either that the parameters in the source region are quite different from what is currently considered

plausible or that RPE due to Langmuir waves generated in a beam instability is not the emission mechanism. Let us consider whether it is possible for the parameters to be modified in such a way that the predicted frequency in equation (42) is compatible with observed frequencies. Suppose the plasma density were not much different from the Goldreich-Julian value (the multiplicity $M \sim 1$) and that the plasma is only mildly relativistic (all γ 's of order unity). Then the frequency in equation (42) is of order the observed frequencies for r/R_* in the plausible range $10\text{--}10^2$. Could the radio emission arise in such anomalously low-density mildly relativistic regions, presumably at the edges of the bulk of the outflowing relativistic plasma? There is some support for this suggestion from the interpretation of the polarization of pulsar radio emission by von Hoensbroech, Lesch, & Kunzl (1998), who found that the data are compatible with a model in which the background plasma is essentially cold and of one predominant sign of charge in its rest frame. However, there is no theoretical basis for such a model, and it seems more plausible to consider alternative emission mechanisms that are compatible with existing polar-cap models than to seek to modify the model in such a drastic way.

The remaining possibility for RPE due to a beam instability is the growth of low-frequency ($\omega \ll \omega_1$) Alfvén waves. However, the resonance condition for the growth of Alfvén waves due to a beam instability cannot be satisfied in the polar-cap regions for seemingly plausible parameters (see eq. [45]). An exception is for an instability due to extremely energetic particles, such as the beam of primary particles. However, a further difficulty arises with this suggestion, in that the growth rate increases with increasing frequency, favoring waves with frequencies comparable to ω_1 and so encountering the same incompatibility with observations as for Langmuir waves. Moreover, the instability for Alfvén waves with a beam of given energy occurs at one specific height, requiring that all frequencies be emitted from essentially the same height. Although this is not excluded by observations, the interpretation of the data in terms of a radius-to-frequency mapping seems much more plausible.

The simplest interpretation of these results is that RPE due to a beam instability, in either Langmuir waves or Alfvén waves, is not the pulsar emission mechanism. The other pulsar emission mechanisms mentioned in § 1 need to be reconsidered critically to see which of these remain viable when they are analyzed in a similar critical way.

Another general conclusion is that whatever the emission mechanism is, it must produce radiation at well below the frequency of the subluminal Langmuir waves. Of the possible waves, only superluminal L-O mode and magnetoacoustic waves can escape from the plasma. In either case, the escaping radiation would be entirely in the one mode that is linearly polarized. This can account for the well-known sweep of the linear polarization in the single-vector model of Radhakrishnan & Cooke (1969), but it cannot explain the rich variety of other observational features relating to polarization. Thus a further implication is that other features of the observed polarization must be imposed as a propagation effect, perhaps when the radiation passes through the region where it is in cyclotron resonance with the particles in the plasma (e.g., Mikhailovskii et al. 1982).

D. B. M. thanks Simon Johnston, Qinghuan Luo, and Andrew Willes for helpful comments on the manuscript.

REFERENCES

- Allen, M. C., & Melrose, D. B. 1982, *Proc. Astron. Soc. Australia*, 4, 365
- Arons, J. 1983, *ApJ*, 266, 215
- Arons, J., & Barnard, J. J. 1986, *ApJ*, 302, 120
- Asséo, E. 1993, *MNRAS*, 264, 940
- . 1995, *MNRAS*, 276, 74
- Asséo, E., & Melikidze, G. I. 1998, *MNRAS*, 301, 59
- Asséo, E., Pellat, R., & Rosado, M. 1980, *ApJ*, 239, 661
- Asséo, E., Pellat, R., & Sol, H. 1983, *ApJ*, 266, 201
- Benford, G., & Buschauer, R. 1977, *MNRAS*, 179, 189
- Beskin, V. S., Gurevich, A. V., & Istomin, Ya. N. 1988, *Ap&SS*, 146, 205
- Cheng, A. F., & Ruderman, M. A. 1977, *ApJ*, 212, 800
- Chugunov, Yu. V., & Shaposhnikov, V. E. 1988, *Astrophysics*, 28, 98
- Egorenkov, V. D., Lominadze, D. G., & Mamramdze, P. G. 1983, *Astrofizika*, 19, 753
- Gedalin, M. E., & Machabeli, G. Z. 1983, *Astrofizika*, 19, 91
- Gedalin, M., Melrose, D. B., & Gruman, E. 1998, *Phys. Rev. E*, 57, 3399
- Ginzburg, V. L., Zheleznyakov, V. V., & Zaitsev, V. V. 1969, *Ap&SS*, 4, 464
- Godfrey, B. B., Newberger, B. S., & Taggart, K. A. 1975, *IEEE Trans. Plasma Sci.*, PS-3, 60
- Godfrey, B. B., Shanahan, W. R., & Thode, L. E. 1975, *Phys. Fluids*, 18, 346
- Hardee, P. E., & Rose, W. K. 1976, *ApJ*, 210, 533
- . 1978, *ApJ*, 219, 274
- Harding, A. K., & Muslimov, A. G. 1998, *ApJ*, 508, 328
- Hinata, S. 1976a, *ApJ*, 203, 223
- . 1976b, *ApJ*, 206, 282
- Kaplan, S. A., & Tsytovich, V. N. 1973, *Plasma Astrophysics* (Oxford: Pergamon)
- Kazbegi, A. Z., Machabeli, G. Z., & Melikidze, G. I. 1987, *Australian J. Phys.*, 40, 755
- . 1991, *MNRAS*, 253, 377
- Kijak, J., & Gil, J. 1998, *A&A*, 299, 855
- Kramer, M., Xilouris, K. M., Lorimer, D., Doroshenko, O., Jessner, A., & Lyne, A. G. 1997, *A&A*, 322, 846
- Kroll, N. M., & McMullin, W. A. 1979, *ApJ*, 231, 425
- Kunzl, T., Lesch, H., Jessner, A., & von Hoensbroech, A. 1998, *ApJ*, 505, L139
- Larroche, O., & Pellat, R. 1987, *Phys. Rev. Lett.*, 59, 1104
- Lominadze, D. G., Machabeli, G. Z., Melikidze, G. I., & Pataraya, A. D. 1986, *Soviet J. Plasma Phys.*, 12, 712
- Lominadze, D. G., Machabeli, G. Z., & Usov, V. V. 1983, *Ap&SS*, 90, 19
- Lominadze, D. G., & Mikhailovskii, A. B. 1979, *Soviet Phys.—JETP Lett.*, 49, 483
- Lominadze, D. G., Mikhailovskii, A. B., & Sagdeev, R. Z. 1979, *Soviet Phys.—JETP Lett.*, 50, 927
- Luo, Q., & Melrose, D. B. 1992, *MNRAS*, 258, 616
- . 1995, *MNRAS*, 276, 372
- Luo, Q., Melrose, D. B., & Machabeli, G. Z. 1994, *MNRAS*, 268, 159
- Lyubarskii, Yu. E. 1992, *A&A*, 265, L33
- . 1993, *Soviet Astron. Lett.*, 19, 208
- Lyutikov, M. 1998, *MNRAS*, 293, 447
- Machabeli, G. Z., & Usov, V. V. 1989, *Soviet Astron. Lett.*, 15, 393
- . 1978, *ApJ*, 225, 557
- . 1981, in *Pulsars*, ed. W. Sieber & R. Wielebinski (Dordrecht: Reidel), 133
- Melrose, D. B., Gedalin, M. E., Kennett, M. P., & Fletcher, C. S. 1999, *J. Plasma Phys.*, in press
- Melrose, D. B., & Stoneham, R. J. 1977, *Proc. Astron. Soc. Australia*, 3, 120
- Mikhailovskii, A. B., Onischenko, O. G., Suramlishvili, G. I., & Sharapov, S. E. 1982, *Soviet Astron. Lett.*, 8, 369
- Radhakrishnan, V., & Cooke, D. J. 1969, *Astrophys. Lett.*, 3, 225
- Rowe, E. T. 1992, *Australian J. Phys.*, 45, 1 & 21
- . 1995, *A&A*, 269, 275
- Ruderman, M. A., & Sutherland, P. G. 1975, *ApJ*, 196, 51
- Shaposhnikov, V. E. 1981, *Astrophysics*, 17, 407
- Shibata, S., Miyazaki, J., & Takahara, F. 1998, *MNRAS*, 295, L53
- Sturrock, P. A. 1971, *ApJ*, 164, 529
- Suvorov, E. V., & Chugunov, Yu. V. 1973, *Ap&SS*, 23, 189
- . 1975, *Astrofizika*, 11, 305
- Tsytovich, V. N., & Kaplan, S. A. 1972, *Astrophysics*, 8, 260
- Usov, V. N., & Usov, V. V. 1988, *Ap&SS*, 140, 325
- Usov, V. V. 1987, *ApJ*, 320, 333
- Volokitin, A. S., Krasnoselskikh, V. V., & Machabeli, G. Z. 1985, *Soviet J. Plasma Phys.*, 11, 531
- von Hoensbroech, A., Lesch, H., & Kunzl, T. 1998, *A&A*, 336, 209
- Weatherall, J. C. 1994, *ApJ*, 428, 621
- Zheleznyakov, V. V., & Shaposhnikov, V. E. 1979, *Australian J. Phys.*, 32, 49